The use of 3D-printers as plotters opens up a new world in performing 2D migration analyses

Hanjo Köppe[1,2, §], Magnus G. Richert[3], Debora Singer[6,7], Jorn Köppe[4], Mattes Köppe[5], Mladen Tzvetkov[1], Henry W. S. Schroeder[2], Sander Bekeschus[6,7, *], Sandra Bien-Möller[1,2, *]

[1]Department of General Pharmacology, University Medicine Greifswald, 17475 Greifswald, Germany
[2]Department of Neurosurgery, University Medicine Greifswald, 17475 Greifswald, Germany
[3]Technical University of Darmstadt, 64277 Darmstadt, Germany
[4]Technical University of Applied Sciences Lübeck, 23562 Lübeck, Germany
[5]Drägerwerk AG & Co. KGaA, 23558 Lübeck, Germany
[6]ZIK plasmatis, Leibniz Institute for Plasma Science and Technology (INP), 17489, Greifswald, Germany
[7]Clinic for Dermatology and Venerology, Rostock University Medical Center, 18057, Rostock, Germany
[*]These authors contributed equally
[§]Corresponding author

Corresponding Author: Hanjo Köppe
Institute of Pharmacology/C_DAT
Clinic for Neurosurgery
University Medicine Greifswald
Felix-Hausdorff-Str. 3
17487 Greifswald, Germany
Email: hanjo.koeppe@stud.uni-greifswald.de

Abstract:

Scratch wound healing assays remain one of the most commonly used 2D migration assay to obtain a broad overview of the migration behavior of cultured cells. They are easy to perform and cost effective, but yet not standardized in terms of the geometric dimensions of the scratch, e.g. consistency of the scratch width and straightness of the line, especially when performed manually. Furthermore, conventional scratch assays only include a single scratch, which leads to a limited evaluation of a restricted cell population within the culture plates, but not of all cells grown in the chamber. There are commercially available 'scratch-makers' which are highly expensive and yet lack advanced functions such as scratching complex patterns. However, such complex scratch formations would make it possible to assess the entire cell population in a chamber and to evaluate the influence of the scratch itself, e.g. with regard to the regulation of migration-associated proteins. We have therefore developed for the first time a method that not only standardizes the scratch dimensions for different pipette tips, but also gives the opportunity to scratch any conceivable 2D shape by using 3D printers as 2D plotters. This open-source and low-cost system can be performed with any plate format from any manufacture under culture hood conditions. The 2D plotter-based method developed and validated by us provides highly reproducible and consistent scratch parameters for *in vitro* migration analyses.

Introduction

Scratch wound healing assays (scratch assays) are, alongside with cell exclusion methods, the most frequently used 2D migration assays for evaluating the migration behavior of cells *in vitro*. For this, cells are cultured until they reach confluence and then separated by pulling a pipette tip through the monolayer to create a gap (scratch) with two facing wound edges (1,2). This is usually performed manually which leads to a highly inconsistent wound morphology and therefore makes it difficult to compare different experiments with each other. Ensuring equal wound diameters is particularly important for the quantification of cell migration behavior after different treatments, as these are regularly compared with a control group and therefore depend on equal scratches in the control group and the intervention group (8). Nevertheless, scratch assays remain a widely used assay with around 12,000 entries in *PubMed* to date, most of which are performed manually. Due to the natural limits of the human hand, manual execution inevitably leads to inconsistencies and irregularities in terms of straightness, contact pressure and pulling speed. The conventional method also lacks the opportunity of a scalable approach, as it is almost impossible to scratch manually within the 96-well plate format. Moreover, complex shapes cannot be implemented manually, although this would allow to induce migration processes in all cells of a well. This would make it possible to investigate the regulation of migration within the cell assembly and to draw conclusions about the regulation of migration-associated proteins, e.g. by immunofluorescence staining after the experiment has been completed. This versatile use of scratch assays underlines the importance of making standardized approaches accessible to the majority and thus achieving an improvement in various fields of science.

Although there are different methods to create equal gaps for migration analyses, none of them fully meets the requirements in terms of cost efficiency, reliability, user-friendliness and scalability (9). For example, cell exclusion assays (5), in which cells are seeded into silicon chambers so that they are separated by a barrier until the chambers are removed to create a gap, are highly versatile but also come with some limitations. This approach is not scalable, as these chambers do not fit into smaller plate formats and are only available in certain geometric dimensions and volumes. In addition, depending on the desired experimental observation, the surrounding cells may not be optimally affected to exactly mimic a ‘scratch

assay'. This could be important if the goal is to simulate, for example, surgical injury or the formation of scars from repeated scratching (10).

There are also some highly functional DIY approaches (3,6,7,11), but most of them are over-engineered and require sophisticated machinery to produce, so they are not reproducible for the majority of scientist. Recently, *Lin et al.* (12) published a similar approach as a preprint. Although this approach also involves low production effort, parts still need to be printed for the setup, which means that the opportunity to use the printer itself as a more direct solution has been missed so far. Furthermore, most DIY machines are tailored to one specific size of cell culture plates and therefore only fulfill a specific need. Some companies also offer commercially available devices that can be used to perform single straight gaps, but these are extremely expensive (around USD 12,000) and thus not suitable for everyone. *Fenu et al.* (13) published an interesting low-cost approach in which they showed that it is possible to reproduce single straight lines with high precision by sliding magnets through the wells, but again it lacks the same capabilities as the cell exclusion inserts. Notably, there are some other methods to perform scratch assays with high accuracy, e.g. thermal ablation of cells within the gap by laser radiation (14,15) or electrical current (16), but all of them have their own disadvantages regarding user-friendliness, effectiveness and low-cost. In consequence, there is a huge need for standardization and automation of the conventional pipette-based scratch assay through an open hardware and software approach.

All of the above-mentioned challenges that the other approaches fail to address, can be solved by using the precise XYZ axis environment which is provided by 3D printers. Linear-guided axes and stepper motors eliminate hand tremor and imprecise tip movements, spring-loaded test tips ensure constant contact, vector graphics enable free-form scratches, and an open-source program for generating G-code allows adjustments to meet individual preferences. We have named our approach **ASAPR**, which stands for **A**dvanced **S**cratch **A**ssay **P**lotting **R**obot. ASAPR offers some significant benefits: (1) any culture plate or culture dish with a lid can be used (up to a certain size), (2) any pipette tip can be used, (3) any 2D shape can be scratched, (4) all device parts with cell contact can be sterilized, (5) the procedure is carried out under a sterile culture hood, (6) the method offers automatic washing steps to avoid cross-contamination (7), the system is programmable to the desired needs (8), it is easy to set up, and (9) requires only minor extra costs besides the 3D printer itself (~15 USD).

Results

Set up and principle of ASAPR on 3D printers

ASAPR can be used with any commercially available 3D printer that supports the execution of 'raw' or 'manual' G-code, which is the case for most models. The idea is to use the 3D printer as a plotter by moving the print head only in the x and y direction while giving the z axis a fixed execution height within the desired culture dish or plate. We therefore developed two different approaches, either by screwing a pipette mount directly into the M6 thread as a replacement for the nozzle (I) or by printing a small attachment for a precision chuck which then holds the pipette tip (II) (Fig. 1C). We recommend approach number (I), as it is easier to determine the needed x and y offsets later (see Methods) and the automatic leveling of the 3D printer is more effective, as the pipette tip is in exactly the same position as the nozzle before. To ensure uniform pressure throughout the whole experiment, we used high-precision spring-loaded test probes, which are normally used for 'in circuit tests'. The end of the tip itself consists of a regular pipette tip, which is cut by a 3D-printed cutting device to ensure a uniform length and then placed on the tip of the spring-loaded test probe. The pipette tip centers itself due to the conical shape of the spring-loaded probe tip (Fig. 1C). To hold the cell culture plates on the printing platform, we designed a 3D-printed mount that clamps downwards (Fig. 1B; data available on GitHub). This mount can be adjusted in size via an adjusting screw to allow the plates to be clamped tightly. Other mounts, e.g. for dishes, will be released in the future on GitHub. At this point, the mechanical setup is already complete, and the first G-code can be generated using the provided program 'ASAPR' (Fig. 1A, for setting up the possibility to include washing steps see GitHub).

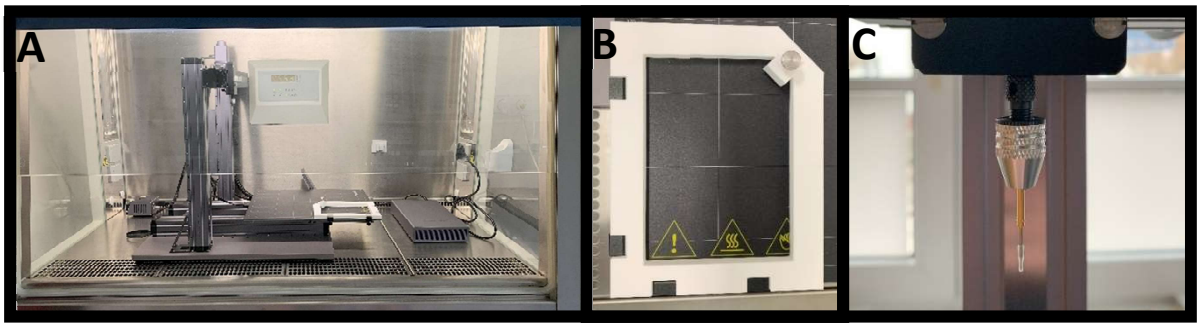

Figure 1. Set up ASAPR on 3D printers.

(A) The setup can even be used with large 3D printers under a sterile culture hood and is easy to disinfect using UV disinfection. Quick assembly is guaranteed and can also be easily removed. (B) The 3D-printed plate holder is clamped onto the printing platform and enables the cell culture plates to be clamped firmly in the same position. (C) Illustration of how the pipette tip is attached using a precision chuck that is pressed into a 3D-printed adapter. The chuck contains a spring-loaded test tip to ensure equal contact with a cut to size pipette tip, which is the only part that later comes into contact with the cells.

Generation of an appropriate G-code

The print head does not automatically know on which section of the printing platform the cell culture plate is located. For this purpose, the offsets of the x- and y-axis must first be determined in order to specify the maximum frame within which the print head may later operate. The z-axis offset must also be determined so that the tip acts at the correct depth, although this does not have to be as precise as in the x and y directions, as the spring-loaded tip compensates for unevenness in conjunction with the printer's autoleveling function. It is highly recommended to take your time to determine the offsets very carefully, as you only need to determine them once and they will always remain the same for the device afterwards (for full calibration see GitHub). G-code works in a similar way to a series of directional instructions in a three-dimensional coordinate system. To generate these instructions, we have written our own program in Python 'ASAPR'. This program provides a variety of functions and offers three different patterns. The *Mesh* pattern only executes straight lines, which can be placed at any distance from each other and can therefore also be used for individual scratches. These can also be tilted by 90 degrees to create a grid. The *Circle* pattern is used to scratch circles increasing in size into larger cavities to encourage all cells in a well to migrate. The *SVG* pattern makes it possible to scratch any conceivable .svg file, i.e. vector graphics, by automatically scaling them to the size of the wells. Vector graphics can be created beforehand using open source software such as Inkscape. The G-code can then either be transferred to the 3D printer via USB stick or executed directly via W-LAN. The geometric dimensions of the plate to be processed can be taken from the data sheet and are loaded into the program via a text file, which allows the use of many plate types and quick adjustments to the orientation by swapping x and y (the exact options are discussed on GitHub).

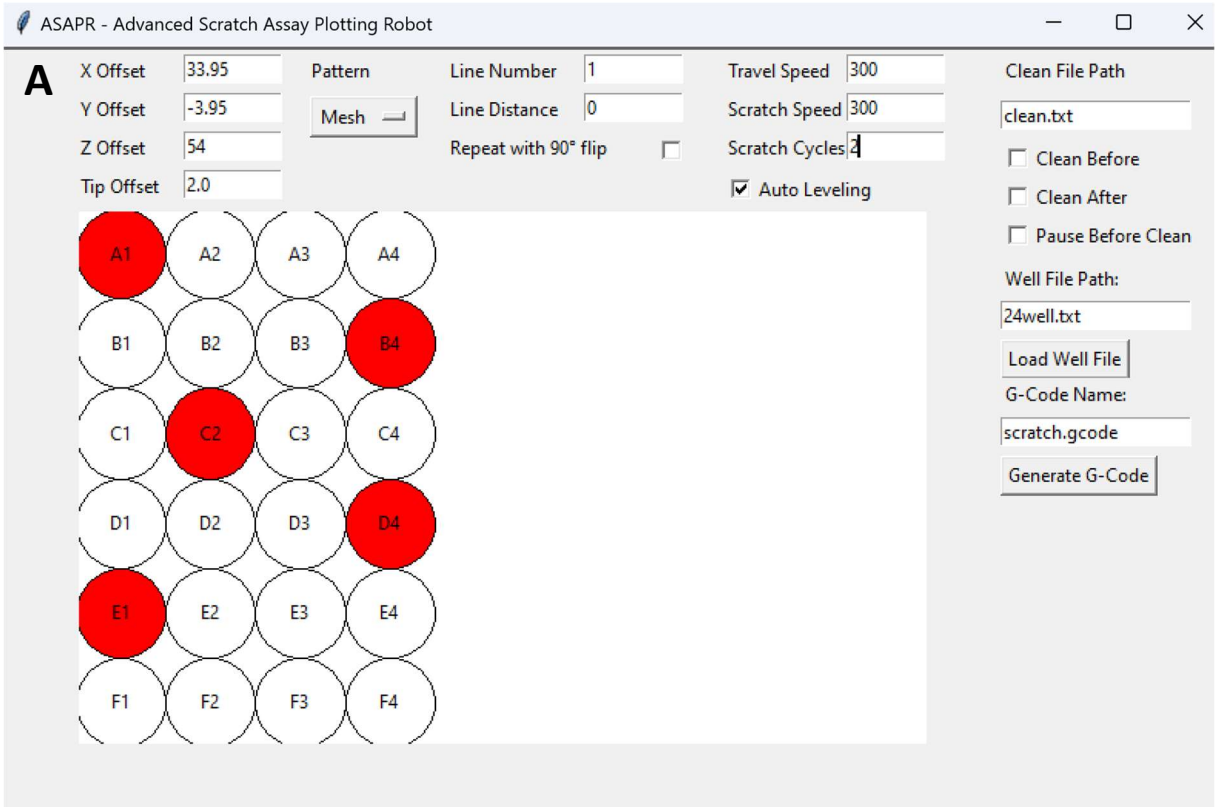

Figure 2. G-code generating program.
(A) An example representation for the generation of the G-code for individual straight scratches within a 24-well plate. A safety distance of 2 mm to the edges of the well is set via the 'Tip Offset' task function. The running and scratch speed are set to 300 mm/s, which has proven to be optimal. The scratch movement runs back and forth to achieve the straightest possible wound edges, which is set via 2 'Scratch Cycles'. Wells of the culture plate that are not required (here A1, B4, C2, D4 and E1) were omitted by clicking on them and are then not included in the code. After generation, the code is saved in the same folder as the graphical user interface (GUI).

Validation of single scratch reproducibility

We first validated the reproducibility of standard single straight lines, as mostly performed using conventional scratch assays. A total of three 24-well plates were processed, so that 72 scratches were included for single scratch validation. The scratching experiments were carried out on the glioblastoma cell line LN-18. Optimal conditions were found to be 100% confluence, short incubation times to minimize cell-cell adhesion and cell-surface adhesion, scratch speeds of 300 mm/s and using two 'Scratch Cycles'. To ensure reproducibility, we focused on the parameters wound width and wound area, whereby the standard deviation of the wound width can also be used to assess the straightness of the lines. Our approach revealed a coefficient of variation of 1.61% for wound area and wound width (Fig. 3A) with a perfect correlation (r = 0.99) between each other indicating a rectangular shape. A comparison with self-performed manual scratching does not appear to be expedient, as the subjective bias

would be too significant for this, which is why reference is only made here to the published literature for comparison. Based on the published data on the accuracy of manually performed scratch assays, the coefficient of variation is approximately 8-17% for the gap width and about 6% for the straightness of the line (13,17).

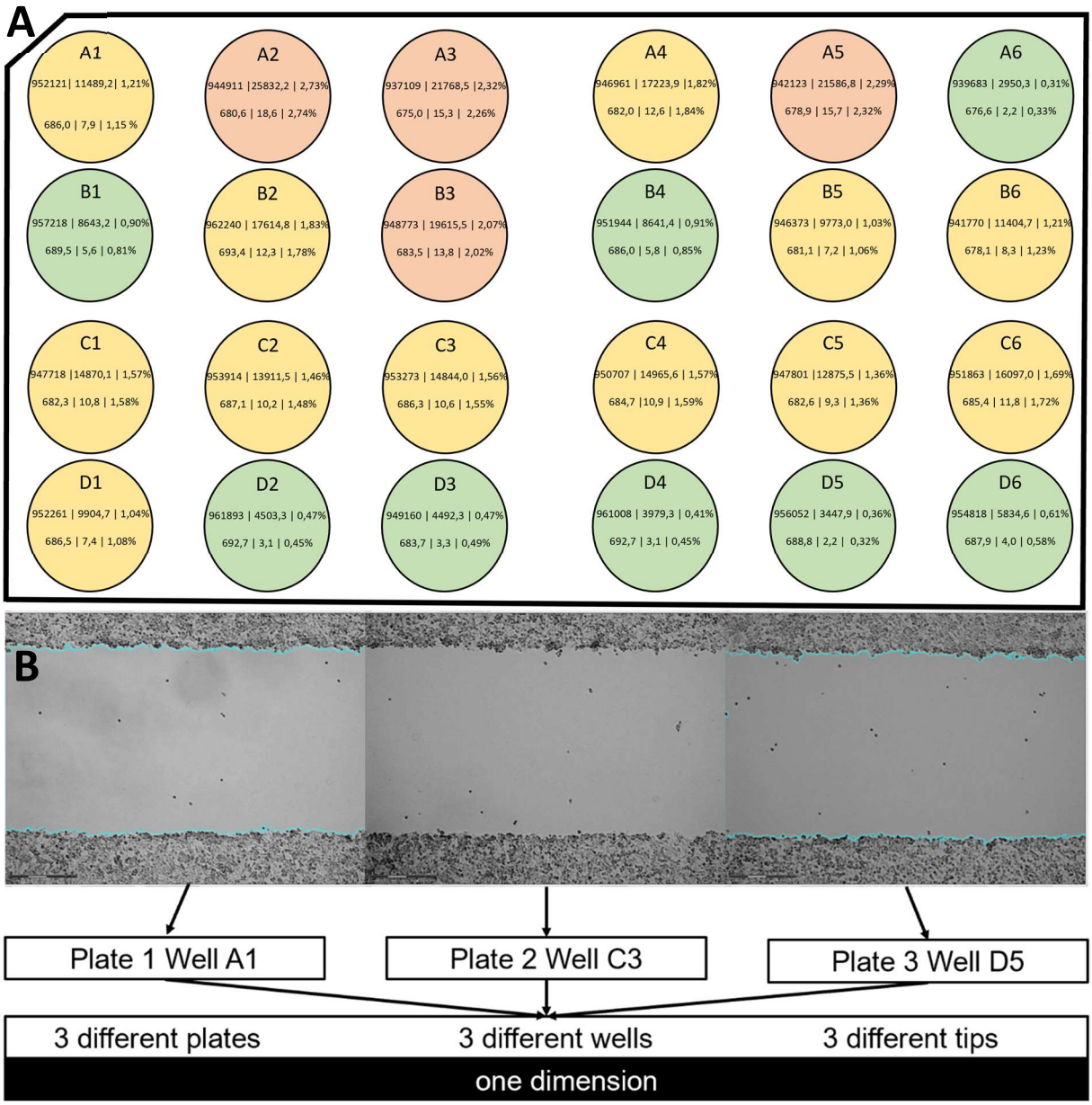

Figure 3. Single Scratch validation.
(A) The heatmap shows the consistency in making single straight scratches in 24-well plates cultured with the glioblastoma cell line LN-18 using ASAPR. All scratches were generated using the modular 3D printer *Snapmaker® A350* with a 200 µl pipette mounted. Each image was taken randomly across the scratches on the first plate, and the position was then marked to be viewed on the other two plates as well. No shift in the localization was detected in the other scratches. For each well, the mean value of the cell-free area, the standard deviation of the cell-free area and the coefficient of variation (CV) value of the cell-free area as well as the gap width are shown in the heatmap above. Green wells represent a CV under 1%, yellow wells have a CV of 1-2% and red wells show a CV of more than 2% for the mean gap area and mean gap width, as they correlate perfectly with each other. The area is given in pixels² and width in pixels. (B) Representation of three example scratches from three different wells of three different plates, all created with ASAPR. The images were taken using brightfield microscopy. Scale bar: 300 µm.

Validation of complex two-dimensional shapes

The study of complex scratch patterns is particularly interesting because it allows for the investigation of the influence of scratch morphology itself on migration behavior (18). Additionally, when combined with live cell imaging, it becomes also possible to observe not only a small section but the entire well, which hopefully leads to more precise overall results and is impossible to perform manually (21). The G-code generating program creates a toolpath similar to that of a laser engraver and then follows it. As a result, the smallest possible details also depend on the size of the pipette tip used. The tip widths are approximately: 1000 µl - 1.2 mm, 200 µl - 0.8 mm, and 10 µl - 0.7 mm.

To validate the scratching of complex two-dimensional shapes, mazes were applied in 6-well plates (Fig. 4A), which were subsequently quantified using immunofluorescence microscopy. For this, LN-18 cells were stained with DiD 24 hours before the scratch was done. The quantification of the cell-free area resulted in a mean area of $4.905*10^8$ µm² and a coefficient of variation of 1.51% for a total of 18 wells with respect to the wound area. Quantifying shape accuracy is challenging, as it would require an approach that overlays all shapes and determines the deviations from the original shape.

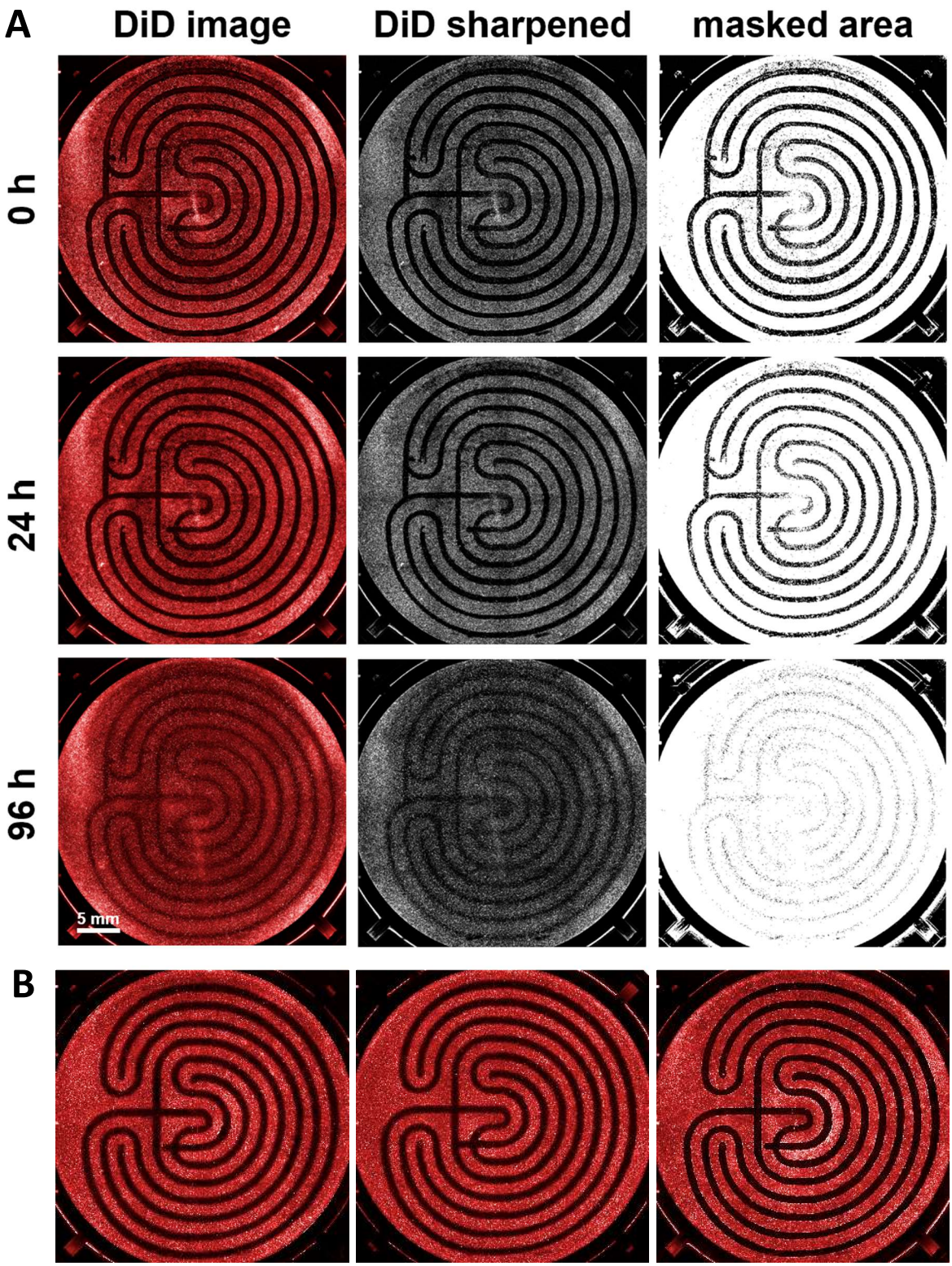

Figure 4. Quantification of complex shapes, e.g. mazes.
(A) The image processing procedure is shown after the immunofluorescence images were recorded by scanning all wells of a 6-well plate. To enhance the distinguishability, the image is first increased in contrast and then only the non-covered area was masked. Over the course of 96 hours, it can be clearly seen how the wound area closes almost completely and uniformly. Scale bar: 5 mm. (B) Three further example images of scratched mazes at time point t=0h, which clearly demonstrate the high replicability.

Induction of migration-associated proteins and cytokines

To stimulate nearly all cells in a 6-well plate to migrate, the wells were treated with a total of 16 individual scratches across the entire width, all equally spaced, resulting in 18 cell bridges of 400 µm width from which the cells migrate left and right to cover the gap (Fig. 5A). While in single scratches only cells near the wound edges migrate, this approach achieves a migration status in almost all cells in response to this large wound area, allowing for subsequent analysis of regulatory mechanism linked to cell damage and migration in most cells. This approach is called the 'Mesh'. After 24 hours of migration, the medium was collected to determine IL-6 secretion by ELISA. Additionally, cells were either harvested for subsequent Western blot analysis or stained with crystal violet to quantify the relative cell number by staining all viable cells. This allowed to compare protein (Fig. 5C) and cytokine (Fig. 5B) levels between migrating and non-migrating cells. In addition to LN-18 cells, the regulation of cytokines and migration-associated proteins was also examined in primary glioblastoma cells (prGBM) in the same experimental setting. The scratched cells showed a significant induction of CD44 and N-Cadherin for both LN-18 and prGBM after 24h of migration, but not for the matrix metalloproteinase-2 (MMP2). The strongest induction was observed for N-cadherin in LN-18 cells, with a 3.5-fold increase after 24 hours. Additionally, the amount of IL-6 secreted per cell was doubled in LN-18 and 2.5-fold increased in prGBM cells 24 hours after the scratch was done. It is important to note that cells were treated with 5 mM hydroxyurea after scratching to determine only migration and not proliferation. Since the aim here is merely to demonstrate a possible application and not to analyze which migration proteins are regulated in glioblastoma cells, the results will not be further explained at this point.

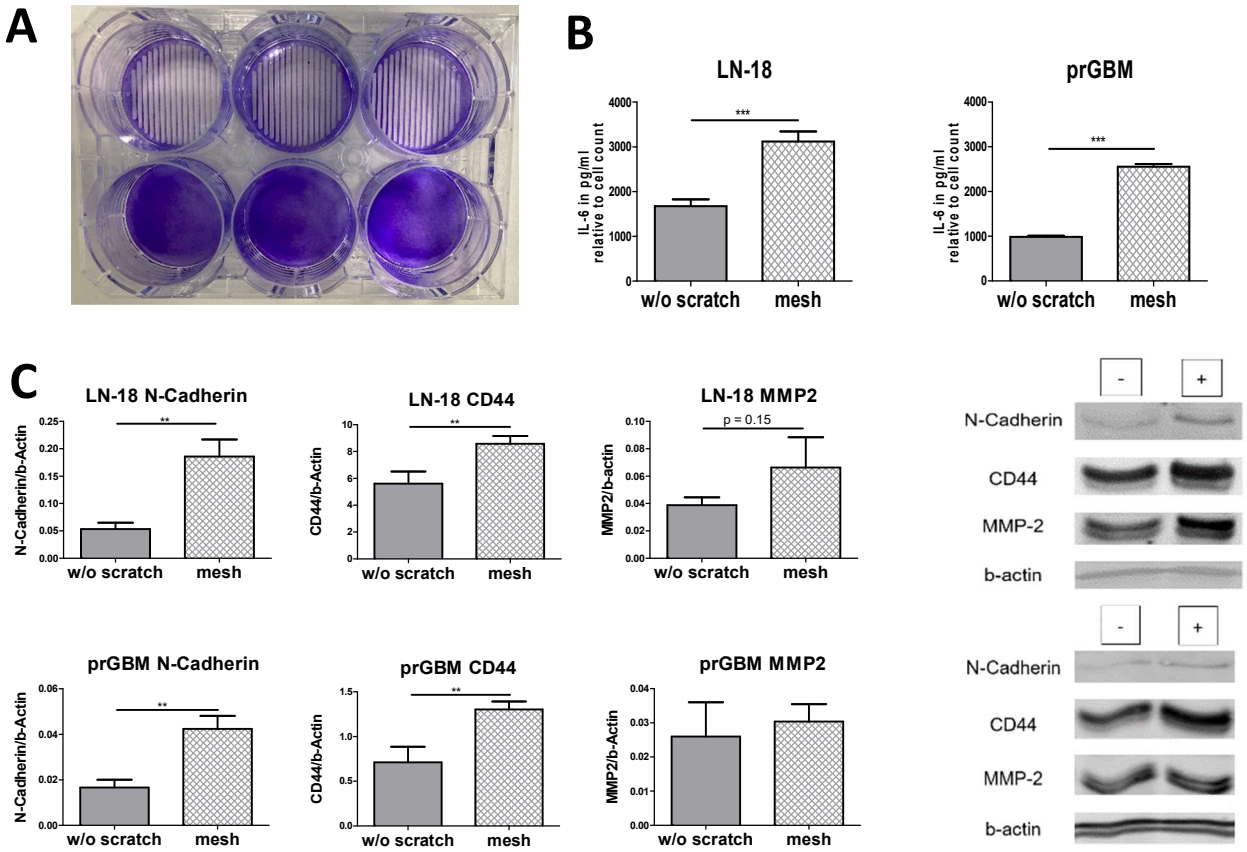

Figure 5. Induction of migration-related proteins and cytokines.
(A) Non-scratched and cells after performing the mesh scratch, subsequently stained with crystal violet. Visible are the 400 µm wide cell bridges, which are evenly arranged across the entire well. (B) To investigate whether migrating cells secrete more IL-6 then non-migrating cells, the cell monolayer of a 6-well plate was scratched over the entire well after the cells have reached confluency using the mesh procedure. The IL-6 concentrations are normalized to the relative cell number within a well by staining all viable cells with crystal violet after removal of the cell supernatant. Mean ± SD, n = 3. Statistical significance was calculated by unpaired, two-tailed t-test. *p ≤ 0.05, ** p ≤ 0.01, *** p ≤ 0.001. (C) After 24h of migration, the cells were harvested and protein was isolated for Western blot. We investigated the migration-related proteins CD44, MMP-2 (Matrix-Metalloproteinase 2) and N-Cadherin. '-'indicates unscratched and '+' scratched cells. Mean ± SD, n = 3. Statistical significance was calculated by unpaired, two-tailed t-test. *p ≤ 0.05, ** p ≤ 0.01, *** p ≤ 0.001.

Discussion

We have established and validated a 2D printer-based method that provides highly reproducible and consistent scratch parameters for in vitro migration analyses. During the test phase, numerous sources of error emerged that should be taken into account when using ASAPR. Many of these approaches are also important for improving conventional scratch assays. The area to be scratched should be considered as an elastic sheet that adheres to a surface. If the cells are too tightly connected to each other, more neighboring cells will be pulled out than just those that should be lost by scratching with the pipette tip, resulting in

frayed wound edges (19). Conversely, if the cells adhere too strongly to the plate, the pipette tip may not catch all of them, leading to very irregular wound edges (Fig. S1). To eliminate these two disturbances, there are two possible solutions, and both of which should ideally be implemented simultaneously. First, the cells should be given a short adhesion time (optimally no longer than 24 hours) to minimize too close cell-cell and cell-surface contacts (19). Second, the scratch should be made at very high speeds to take advantage of the inertia of the cells adhering to the surface. Additionally, the inertia of the pipette tip increases at higher speeds, which should theoretically lead to less vibration. In this context, it would be very interesting to see what significantly faster printers could achieve, as the *Snapmaker A350*® used here is limited to a maximum of 300 mm/s due to its lead screw mechanism. Core-XY and rail-guided printers, in particular, can reach much higher speeds (22).

A further significant improvement was achieved through the use of spring-loaded test probes. Although most 3D printers have a well-functioning automatic leveling system, it was still common for the cell surface not to be reached at certain points with the same z-value. As the pipette tips themselves are very inflexible, this is an adjustment that is difficult to achieve manually, and it cannot be guaranteed that the same pressure is applied consistently across the surface. This uncertainty in manual scratching was eliminated by using spring-loaded test probes. Although our approach has yielded excellent results, there are still some areas that can be improved. For example, while the spring-loaded test probes have greatly improved the consistency of the pressure applied, their slight but present backlash can lead to irregularities that result in less than optimal outcomes.

The highly precise XYZ-axis environment of 3D printers, which forms the basis of the ASAPR concept, proves to be an ideal framework for the use of scratch assays. It enables much more precise, reproducible and customizable assay configurations than manually performed scratch assays (13, 17). Moreover, this approach opens up a whole new world of possibilities for 2D migration analyses, as the induction of migration by complex scratch patterns enables, for the first time, a simple comparison between migrating and non-migrating cells as well as the analysis of the scratch's own impact. Furthermore, this open-source platform offers a multitude of future opportunities, particularly with regard to software development and improvement of the components used. The time saved by ASAPR is also worth mentioning, as the scratches are not only made faster and more precisely but also consistently in the same location. This is particularly beneficial when capturing images manually, without a live-cell

imager, making the process more convenient because the images can always be taken at the same position. This precise reproducibility, even in terms of spatial resolution, offers new approaches for migration studies. For example, repetitive scratches could be applied to the same location, which would enable the investigation of pathomechanisms in scar formation or multiple wound damages.

Overall, ASAPR represents an efficient approach that requires minimal production effort, as all components can be manufactured using the 3D printer itself. There are many DIY approaches to perform highly reproducible scratch assays that require production-based 3D printing, each with their own strengths and weaknesses (23,24). The approach by *Lin et al.* (12) is particularly noteworthy as it comes closest to our concept. However, as 3D-printed parts were needed without using the printer itself, a straightforward process was overlooked. With 3D printers becoming more common in many laboratories for various reasons (25), the barrier to entry for ASAPR is relatively low, facilitating the performance of reproducible, precise, and standardized scratch assays with the opportunity for more in-depth migration analyses.

Methods

Cell culture

The human glioblastoma cell line LN-18 (ATCC, Manassas, VA, USA) were used for development and validation of 3D printer-based scratch assays. Further, primary glioblastoma (prGBM) cells from a surgically resected patient sample were used as described by (20). GBM cells were cultured at 37 °C, 95% relative humidity and 5% carbon dioxide fumigation in DMEM supplemented with 10% FCS, 2 mM glutamine and non-essential amino acids. All cell lines were routinely monitored for mycoplasma contamination using a PCR based assay. The cells were plated at a density of 200,00 cells per well in 6-well format or 40,400 cells per well in 24-well format plates and incubated until confluence was reached.

Western Blotting

GBM cells were scraped, transferred to a 1.5 mL tube and centrifuged at 10,000 rpm for 3 min. Afterwards, the cell pellets were resuspended in lysis buffer (50 mM Tris-HCl, 100 mM NaCl, 0.1% Triton X-100 and 5 mM EDTA, pH 7.4) containing 1 mM leupeptin and 1 mM aprotinin and incubated on ice for 30 min, followed by centrifugation at 12,000 rpm for 5 min at 4 °C. The supernatant was used for protein determination, using the BCA method. Subsequently, after denaturation in Laemmli SDS sample buffer at 90 °C for 10 min, 30 µg of protein was separated on 10% SDS polyacrylamide gels. The tank blot system (Bio-Rad, Hempstead, UK) was used for immunoblotting of the separated proteins on Whatman® nitrocellulose membranes, which were then blocked in 5% FCS in Tris-buffered saline containing 0.05% Tween 20 (TBST) for 1 h at room temperature. The membrane was incubated overnight at 4 °C under rotation with the following primary antibodies diluted in TBST (1:1000): mouse anti-CD44 (Cell Signaling Technology, Boston, MA, USA); rabbit anti-MMP2 (Cell Signaling Technology, Boston, MA, USA); mouse anti-N-Cadherin (Cell Signaling Technology, Boston, MA, USA) and mouse anti-b-Actin (Santa Cruz Biotechnology, Inc., Heidelberg, Germany). Afterwards, the membrane was rinsed three times with TBST for five minutes each time, followed by incubation with the secondary fluorescence-labeled antibody for one hour at room temperature with gentle shaking: anti-mouse IRDye® 680 or 800 CW or anti-rabbit IRDye® 680 or 800 CW (all from Li-cor Bioscience GmbH, Bad Homburg, Germany). After incubation, the membrane was rinsed with TBST three times for five minutes each time at room temperature on a horizontal shaker. Fluorescence signals were detected using the

Odyssey® CLx Imaging System (Li-cor Bioscience GmbH, Bad Homburg, Germany). The relative fluorescence intensities of the specific bands were calculated and normalized to beta-Actin as a loading control.

ELISA for IL-6

The supernatant of the cultured GBM cells was transferred to a 1.5 ml tube, centrifuged at 1,000 rpm for 3 min and pipetted into a new 1.5 ml tube to remove debris. Afterwards the samples were stored at -80°C until measurement. Before measurement, the samples were diluted 1:10 to stay within the calibration curve. The concentrations of IL-6 in the supernatants were determined using ELISA kits (D6050, R&D Systems, USA), according to the manufacturer's instructions.

Analyses of Cell Vitality (Crystal Violet Staining)

The supernatant was aspirated from scratched and control cells, and adherent cells were rinsed once with PBS. Afterwards, cells were fixed in 4% paraformaldehyde for 10 min, followed by gently rinsing three times with PBS. 300 µl of a 0.5% crystal violet staining solution (Sigma-Aldrich Co., Deisenhofen, Germany) was added to the cells and the plates were incubated at room temperature for 10 min. The cells were then washed several times with A. dest. until the dye stopped coming off. After washing, the plate was carefully tapped on filter paper to remove any remaining liquid. Finally, the stained cells were treated with 300 µL SDS solution (1%) and incubated on a shaker for 10 min to dissolve the dye. The optical density was determined at 560 nm (OD560) using a multiplate reader for a total of 36 flashes across each well (Tecan Infinite M200, Crailsheim, Germany).

Scratch configuration

The scratches for single straight lines were made using the specified parameters in the G-code generating program: tip offset ‘2’, mode ‘Mesh’, line number ‘1’, line distance ‘0’, travel speed ‘300’, scratching speed ‘300’, auto-leveling ‘on’, scratch cycles ‘2’.

The scratches for the mesh were made with the specified parameters in the G-code generating program: tip offset ‘2’, mode ‘Mesh’, line number ‘18’, line distance ‘1.6’, travel speed ‘300’, scratching speed ‘300’, auto-leveling ‘on’, scratch cycles ‘2’.

The scratches for the maze were made using the specified parameters in the G-code generating program: tip offset ‘2’, mode ‘svg’, svg scale ‘100’, travel speed ‘300’, scratching

speed '300', auto-leveling 'on', scratch cycles '2'. The svg file is displayed in the supplementary data.

Post-scratch Processing

After scratching, the culture medium was removed and the cells were washed three times with PBS to remove detached cells and prevent their reattachment. When migration was to be observed for 24h, pre-warmed culture medium containing 10% FCS and 5 mM hydroxyurea as a proliferation inhibitor was added.

Microscopic Evaluation

Single straight wounds were imaged using the PALM Robo software of the AxioVision HXP 120C microscope with a 5X objective and a 40X ocular (Carl Zeiss Microscopy, Jena, Germany), and the exact position of the scratches was saved to analyze the same area after incubation. Fluorescence images were captured using PerkinElmer High-Content-Imaging *Operetta CLS* System (PerkinElmer, Waltham, MA, USA). For this, the cells were stained with DiD (V22887, Thermo Fisher Scientific Inc., Darmstadt, Germany) 24h before imaging.

Image and statistical analysis

FIJI (https://imagej.net/software/fiji) was used to process all images (ideal contrast and brightness) and to calculate the wound area for the scratch assays using the wound healing plugin of Suarez-Arnedo et al. (4). The analysis of the immunofluorescence images was performed using *Harmony 4.9* (PerkinElmer, Waltham, MA, USA). Statistical analyses were performed using the GraphPad Prism software 5.0 (GraphPad Software, Inc., San Diego, CA, USA). All data were presented as mean ± SD of at least three independent experiments. Pairwise comparisons were performed using Student's t-test. Statistical significances were defined as * $p < 0.05$; ** $p < 0.01$; and *** $p < 0.001$.

ASAPR hardware setup

A detailed explanation of the operating principle of ASAPR, along with a comprehensive calibration and setup guide, can be found on our GitHub. Below is a brief explanation of the approach used for the *Snapmaker A350®* (SNAPMAKER HK LIMITED, Hong Kong). A holder was printed, which was mounted directly onto the X-axis with four M6 screws so that the system can operate without a print head. A precision drill chuck (MBS03, Donau Elektronik GmbH,

Metten, Germany) was inserted into this holder and secured with a set screw. The drill chuck itself held a spring-loaded test probe (2021-B-1.5N-NI-0.8, PTR HARTMANN GmbH, Werne, Germany). A 200 µl pipette tip was used, which was cut to the same length using a 3D-printed device. This cut-off tip is then simply attached to the test probe and centers itself due to its conical shape. The optimal spring travel was set at 1 mm. Additionally, the 3D-printed plate frame was attached with four clamps designed for glass print beds. This frame includes an M3 knurled screw for securely clamping the inserted plates.

Data Availability

All components for printing as well as technical instructions and explanations of the operating principle and setup are available on the project's GitHub page (https://github.com/MagnusRichert/ASAPR). We are happy to assist with any queries or questions.

Conflicts of Interest

The authors declare no conflict of interest.

Supplementary Information

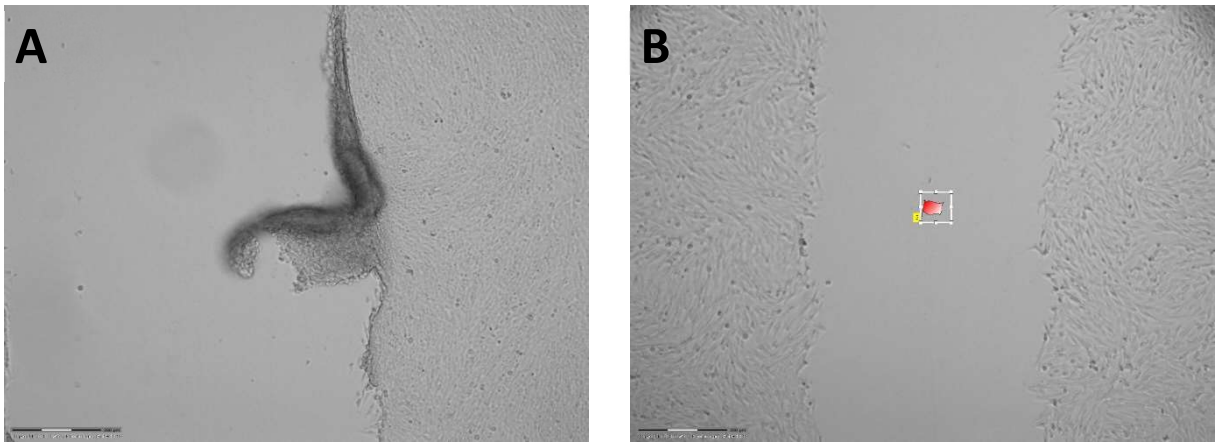

Figure S1: Uneven scratches.
(A) Shown is a failed scratch due to excessively strong cell-cell contacts. It is clearly visible how an entire layer of cells has detached while maintaining contact with the wound edge. (B) Clearly visible irregular wound edges as a consequence of excessively strong cell-surface contacts. Scale bar: 300 µm.

References

1. Liang CC, Park AY, Guan JL. In vitro scratch assay: a convenient and inexpensive method for analysis of cell migration in vitro. Nat Protoc. 2007;2(2):329-333.

2. Martinotti S, Ranzato E. Scratch Wound Healing Assay. Methods Mol Biol. 2020;2109:225-229.

3. Gough W, Hulkower KI, Lynch R, et al. A quantitative, facile, and high-throughput image-based cell migration method is a robust alternative to the scratch assay. J Biomol Screen. 2011;16(2):155-163.

4. Suarez-Arnedo A, Torres Figueroa F, Clavijo C, Arbeláez P, Cruz JC, Muñoz-Camargo C. An image J plugin for the high throughput image analysis of in vitro scratch wound healing assays. PLoS One. 2020;15(7):e0232565.

5. Shiode Y, Morizane Y, Matoba R, et al. A novel cell exclusion zone assay with a barrier made from room temperature vulcanizing silicone rubber. PLoS One. 2017;12(12):e0190198.

6. Chen S, Bin Abdul Rahim AA, Mok P, Liu D. An effective device to enable consistent scratches for in vitro scratch assays. BMC Biotechnol. 2023;23(1):32.

7. Grimmig R, Babczyk P, Gillemot P, Schmitz K-P, Schulze M, Tobiasch E. Development and Evaluation of a Prototype Scratch Apparatus for Wound Assays Adjustable to Different Forces and Substrates. Applied Sciences. 2019; 9(20):4414.

8. Nyegaard S, Christensen B, Rasmussen JT. An optimized method for accurate quantification of cell migration using human small intestine cells. Metab Eng Commun. 2016;3:76-83.

9. Radstake WE, Gautam K, Van Rompay C, et al. Comparison of in vitro scratch wound assay experimental procedures. Biochem Biophys Rep. 2023;33:101423.

10. Nikolić DL, Boettiger AN, Bar-Sagi D, Carbeck JD, Shvartsman SY. Role of boundary conditions in an experimental model of epithelial wound healing. Am J Physiol Cell Physiol. 2006;291(1):C68-C75.

11. Acosta S, Canclini L, Galarraga C, Justet C, Alem D. Lab-made 3D printed stoppers as high-throughput cell migration screening tool. SLAS Technol. 2022;27(1):39-43.

12. Lin Y, Silverman-Dutz A, Bailey M, Cohen DJ. SCRATCH: A programmable, open-hardware, benchtop robot that automatically scratches cultured tissues to investigate cell migration, healing, and tissue sculpting. bioRxiv 2024.08.27.609782. doi: https://doi.org/10.1101/2024.08.27.609782

13. Fenu M, Bettermann T, Vogl C, et al. A novel magnet-based scratch method for standardisation of wound-healing assays. Sci Rep. 2019;9(1):12625.

14. Mathioudaki E, Rallis M, Politopoulos K, Alexandratou E. Photobiomodulation and Wound Healing: Low-Level Laser Therapy at 661 nm in a Scratch Assay Keratinocyte Model. Ann Biomed Eng. 2024;52(2):376-385.

15. Wu SY, Sun YS, Cheng KC, Lo KY. A Wound-Healing Assay Based on Ultraviolet Light Ablation. SLAS Technol. 2017;22(1):36-43.

16. Keese CR, Wegener J, Walker SR, Giaever I. Electrical wound-healing assay for cells in vitro. Proc Natl Acad Sci U S A. 2004;101(6):1554-1559.

17. Jin W, Shah ET, Penington CJ, McCue SW, Chopin LK, Simpson MJ. Reproducibility of scratch assays is affected by the initial degree of confluence: Experiments, modelling and model selection. J Theor Biol. 2016;390:136-145.

18. Vedula SR, Leong MC, Lai TL, et al. Emerging modes of collective cell migration induced by geometrical constraints. Proc Natl Acad Sci U S A. 2012;109(32):12974-12979.

19. Harris AR, Peter L, Bellis J, Baum B, Kabla AJ, Charras GT. Characterizing the mechanics of cultured cell monolayers. Proc Natl Acad Sci U S A. 2012;109(41):16449-16454.

20. Marx S, Wilken F, Wagner I, et al. GD2 targeting by dinutuximab beta is a promising immunotherapeutic approach against malignant glioma. J Neurooncol. 2020;147(3):577-585.

21. Jonkman JE, Cathcart JA, Xu F, et al. An introduction to the wound healing assay using live-cell microscopy. Cell Adh Migr. 2014;8(5):440-451.

22. Wolf J, Werkle KT, Möhring HC. Study on Dynamic Behaviour in FFF 3D-printing with Crossed Gantry Kinematic. Procedia CIRP. Volume 121. 2024. 162-167. https://doi.org/10.1016/j.procir.2023.09.244.

23. Joshi AS, Madhusudanan M, Mijakovic I. 3D printed inserts for reproducible high throughput screening of cell migration. Front Cell Dev Biol. 2023; 11:1256250. Published 2023 Aug 30.

24. Acosta S, Canclini L, Galarraga, et al. Lab-made 3D printed stoppers as high-throughput cell migration screening tool. SLAS Technology. 2022;27(1):39-43

25. Saggiomo V. A 3D Printer in the Lab: Not Only a Toy. Adv Sci (Weinh). 2022;9(27):e2202610.